Analysis of Flooding Effects on the Msingi Masonry Arch Bridge in Mkalama, Singida, Tanzania

[1,2]Dickson Barthazar*, [2]Zacharia Katambara and [2]Gislar Kifanyi

[1]District Office, Tanzania Rural and Urban Roads Agency, P. O Box 725, Sumbawanga, Tanzania

[2]Department of Civil Engineering, Mbeya University of Science and Technology, P.O Box 131, Mbeya, Tanzania

ARTICLE INFORMATION

ABSTRACT

Human induced hydraulic factors have emerged as the leading cause of bridge failures since the 1990s, accounting for approximately 50% of incidents recorded in the authors' database. These failures often occur without warning and result in substantial structural damage. With the intensifying impacts of climate change globally and particularly in Tanzania, such events are projected to become more frequent. Among hydraulic causes, flooding poses the most significant risk, primarily through mechanisms like erosion, high hydraulic forces, and sedimentation.This study assesses the vulnerability of the MsingiMasonry Arch Bridge to flooding, examining both immediate and long-term impacts on its structural integrity. It evaluates the bridge's exposure to flood-related hazards and compares the original design discharge capacity of 1497.57 m³/s with the updated estimate of 1777.90 m³/s, revealing a critical under-capacity during peak flows. Based on these findings, the study proposes adaptive strategies to enhance the bridge's flood resilience.Key recommendations include reinforcing embankments with stone retaining walls, raising the bridge elevation to accommodate future flood levels, and redesigning piers with upstream V-shaped walls to reduce debris accumulation. Additionally, the study advocates for community engagement through awareness programs and the preservation of natural riverbank vegetation to mitigate erosion. These measures aim to inform stakeholders and serve as a reference for flood-resilient infrastructure planning in similarly vulnerable regions.

*Corresponding author's e-mail address: balthazaryd@yahoo.com (Barthazar, D)

1.0 Introduction

Flooding poses a significant threat to infrastructure worldwide, with bridges being particularly vulnerable, especially in regions prone to flooding. In Tanzania, the Msingi masonry arch bridge, located in the Mkalama District of the Singida Region, exemplifies the susceptibility of such infrastructure to flooding. Increasing flood frequency and severity in Tanzania is a result of climatic variability and human-induced factors such as deforestation, urbanisation, and insufficient flood control systems (URT, 2015). These trends raise serious concerns about the stability and longevity of transport infrastructure, which plays a critical role in connecting communities, facilitating commerce, and supporting national development (Migliorini *et al.,* 2020; Jiao *et al.,* 2021).

The failure of bridges due to flooding can lead to widespread economic disruption, limited access to services, and social isolation (Zhao *et al.,* 2019). The Msingi bridge is a crucial link for residents, farmers, and businesses; however, it is situated over a river that is prone to seasonal flooding during the rainy season (Kashaigili *et al.,* 2020). Such floods, a common occurrence in many Tanzanian regions, can rapidly elevate water levels, placing immense stress on nearby infrastructure (Swilla *et al.,* 2024).

Floodwaters can inflict severe damage on bridges through processes like scouring, foundation undermining, and structural weakening (Sharma *et al.,* 2021; Mswada *et al.,* 2020). Scour is a process where fast-flowing water removes soil from around bridge foundations, posing a significant hazard that compromises support structures and increases the risk of collapse (Zhao *et al.,* 2019). This study evaluates the Msingi bridge's vulnerability to such flood-related hazards, including hydraulic forces and sedimentation (Wang *et al.,* 2020; Zhao *et al.,* 2019). Of particular concern are scour and sediment deposition, which can destabilise foundations and accelerate deterioration (Jiao *et al.,* 2021).

The role of climate change is also considered, as future projections suggest increased rainfall intensity and altered river flows that could exacerbate these threats (Nyong *et al.,* 2007). Deforestation compounds this risk by increasing surface runoff, thereby intensifying flood events. Tanzania has experienced alarming rates of forest loss, ranging from 130,000 to over 700,000 hectares annually, due to land conversion for agriculture and fuelwood harvesting (Izidori and Katambara, 2022). This environmental degradation directly contributes to the hydraulic pressures that undermine bridge structures.

Given these interrelated challenges, the study aims to provide a comprehensive assessment of the Msingi bridge's resilience, identifying both current vulnerabilities and potential future risks. It also explores strategies for improving durability, including erosion control, flood mitigation infrastructure, and climate-adaptive design features (Migliorini *et al.,* 2020; Sharma *et al.,* 2021; Gerges *et al.,* 2020).

2.0 Study Area and Methodology

2.1 Description of the Study Area

The Msingi Masonry Arch Bridge spans a total length of 45 m and is located at coordinates 34.33'53.30" East and 4.19'41.31" South in Msingi Ward, along the Nduguti-Ndala-Msingi Road. It is approximately 18.2 km from Nduguti Township, the administrative centre of Mkalama District in the Singida Region. The bridge crosses the Wae River, which originates from the Hanang Highlands in the Manyara Region (Figure 1). The upstream watershed covers an area of 64.664 km². The region is characterised by a dry climatic zone with some agricultural activities being practised adjacent to the river.

2.2 Methodology

This study employed a multidisciplinary methodology integrating structural surveys, geospatial analysis, hydrological modelling, and soil mechanics to evaluate the vulnerability of the Msingi Masonry Arch Bridge to flooding.

2.2.1 Field-Based Structural Assessment

High-resolution digital photography was used to document visible signs of structural distress, including cracks, spalling, and erosion (Rezaizadeh *et al.,* 2011). Measurements of key bridge components (span, arch rise, and pier dimensions) were taken using measuring tapes with millimetre-level precision. The images were geo-referenced and integrated into GIS for spatial analysis. The scour effect was also observed around the bridge's structural elements.

2.2.2 Geospatial Positioning and Terrain Mapping

GPS was used to geolocate the bridge coordinates, which were then integrated into Global Mapper Software. This facilitated the development of high-resolution digital elevation models (DEM), watershed delineation, and the identification of hydrological pathways. TARURA shapefiles were layered to assess the connectivity of the bridge within the regional road network and potential flood-prone zones (Clarke, 2013).

2.2.3 Soil Strength and Erosion Analysis

A Dynamic Probing Light (DPL) test was conducted to evaluate subsurface conditions around the foundation (Jones, 2015; Smith, 2017). Soil resistance was quantified through penetration depth per hammer blow. The scour depth was estimated using the empirical formula proposed by Ferguson and Church (2004) (Equation 1), supported by velocity calculations derived from Manning's equation (Equation 2).

$$d_{sc} = k \times D \times \frac{v^2}{2g} \qquad (1)$$

Where:

d_{sc} = maximum scour depth (m),

k = empirical coefficient between 1.0 and 1.5, depending on the structure and site conditions,

D = diameter of the pier or the width of the structure (m),

V = velocity of the flow at the structure (m/s),

g = gravitational acceleration ($9.81 m/s^2$) and

n = exponent 0.5, depending on the flow conditions and sediment type.

Figure 1

Location of the Study Area and the Upstream Sub-Catchment
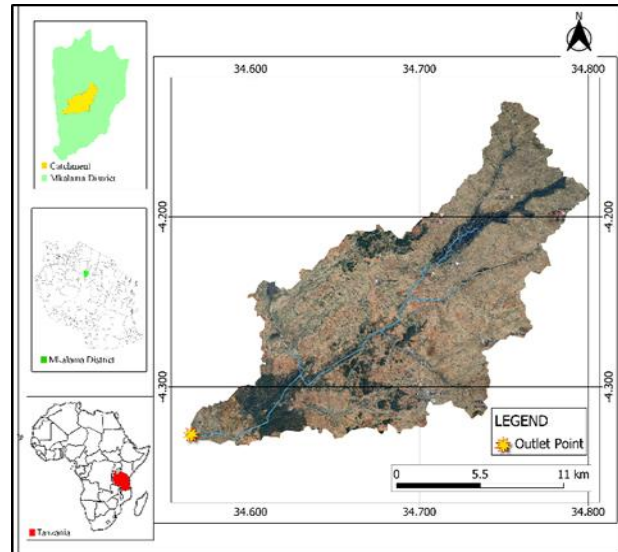
$$v = \frac{1}{n} R^{\frac{2}{3}} S^{\frac{1}{2}} \qquad (2)$$

Where:
S= slope
R= Hydraulic radius
n = Manning factor for concrete bed

2.2.4 Hydrological Modelling Using the TRRL Method

Catchment hydrology was analysed using the TRRL East African Flood Model (EAFM). Data inputs included catchment area, slope, land use, rainfall, and soil type. Storm rainfall intensity was derived from TRRL Report 623 using a 100-year, 24-hour rainfall estimate of 108 mm (Fiddes, 1976; TRRL, 1981). Catchment and channel slopes were calculated using elevation profiles generated in Global Mapper.

2.2.5 Peak Flow and Flood Volume Estimation

Runoff volume and average flow were calculated using standard hydrological equations, taking into account initial retention and lag time. A stepwise iterative approach was applied to estimate base time and peak discharge. Catchment-specific coefficients, such as the contributing area factor, land use factor, and catchment wetness factor, were incorporated to improve accuracy.

2.2.6 Hydraulic Design and Scour Protection

Discharge across the bridge openings was determined using the discharge area and flow velocity relationship. A minimum 1 m flood clearance was permitted. Manning's equation was used to compute critical velocity. Final bridge dimensions were adjusted to accommodate predicted peak discharge and to minimise the possibility of the occurrence of structural vulnerability during flood events.

2.2.7 Structural Simulation and Validation

Prokon Structural Suite was employed to simulate load conditions on the bridge, integrating static, live, and hydraulic forces. Simulations helped assess stress distribution and identify failure modes (Prokon, 2025). Validation was done using field data to ensure model reliability under extreme flood conditions (Katambara, 2020).

2.2.8 Comparative and Climate-Responsive Design Review

Pre- and post-flood bridge conditions were compared using both visual data and hydraulic simulations. Climate variability was taken into account when estimating extreme rainfall scenarios. Recommendations focused on optimising bridge design for long-term resilience, integrating GIS-based flood mapping, and predictive modelling to inform future interventions. This methodology ensures a comprehensive, evidence-based evaluation of the Msingi Bridge, aligning structural, hydrological, and environmental data for resilient infrastructure planning.

Figure 2

Schematic Flow Diagram of the Methodology
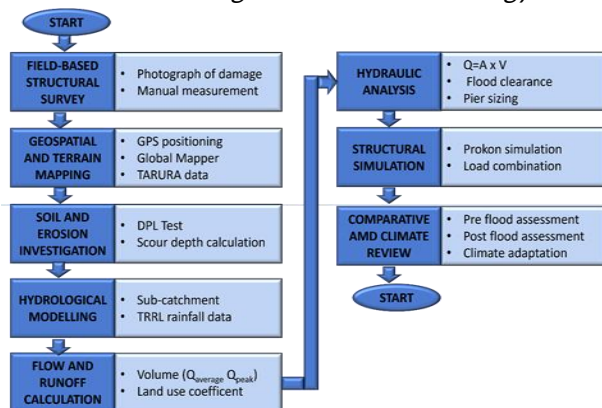
3.0 Results and Discussion

3.1 Observed Field-Based Structural Assessment

Physical surveys, visual inspections, and on-site measurements revealed that the erosion of one of the bridge approaches and the central pier foundation was primarily due to flooding. The existing structure failed to accommodate peak discharge rates during high-flow events, resulting in overtopping and subsequent erosion of the approach embankment (Smith *et al.,* 2020).

The allowable settlement range for masonry arch bridge foundations typically ranges from 45 mm to 90 mm. Exceeding this threshold may compromise structural integrity and lead to failure (Jones & Kumar, 2018). Conversely, settlements below 10 mm typically have minimal impact on load-bearing performance, as the stability factor f remains close to 1. Based on the scouring assessment, the observed settlement due to pier foundation scouring was approximately 5 mm, which is below the allowable limit of 45 mm.

This indicates that the structural integrity of the bridge remains intact. However, observed cracking should be addressed through appropriate repair measures to prevent progressive damage and ensure long-term durability (Cheng & Taylor, 2019).

3.2 Determined Soil Strength and Erosion Outputs

Laboratory and field testing of six geotechnical test pits (P1–P6) yielded safe bearing capacity values of 542.5, 1207.5, 1555.8, 1555.8, 384.2, and 1302.5 kN/m², respectively. Thus, the minimum foundation-bearing capacity recorded was 162.5 kN/m², and the maximum was 1555.8 kN/m². Although some soils exhibited high bearing capacities, they consisted predominantly of sand, a material highly susceptible to hydraulic erosion (USGS, 2025; FHWA, 2001).

On-site measurements recorded a maximum scour depth of 2 m. This value remains below the analytically determined maximum allowable scour depth of 2.6 m. According to guidelines, when actual scour exceeds the allowance, foundation stability becomes critical, and structural failure or collapse becomes feasible (TxDOT, 2018; Ettema

et al., 2010). In this case, the scour depth remains within safe limits, indicating low immediate collapse risk. However, proactive risk mitigation—particularly embankment or pier foundation interventional measures—is advised to guard against potential future exceedance.

3.3 Hydrological Analysis Using TRRL Method

The design flood for the selected catchment in Tanzania was estimated using the empirical approach proposed by the Transport and Road Research Laboratory (TRRL), which has been widely applied in East African hydrological assessments due to its suitability for tropical climates and data-sparse regions (Fiddes, 1976; TRRL, 1981). The methodology relies on key parameters, such as the time to peak (Tp), the catchment lag coefficient (K), and the flood wave attenuation time (Ta), to iteratively compute the base time (Tb) and subsequently, the average and peak discharge.

In the initial iteration, the base time (Tb) was calculated as 1.44 hours using the standard TRRL formula, as recommended for the first iteration in Tanzanian contexts (Ministry of Works, 2007). The total rainfall during the base time was calculated to be 80.2 mm, using the regional rainfall intensity formula adjusted for duration. The Area Reduction Factor (ARF), which accounts for spatial variability in rainfall over the catchment, was determined to be 0.51, leading to an average effective rainfall of 40.9 mm. Given a runoff coefficient of 0.462 and a catchment area of 264.664 km², the total volume of runoff was estimated at 3.63 million m³. This translated into an average discharge of 1,027.1 m³/s. Using a discharge and catchment length of 34,550 m with a channel slope coefficient of 0.38, the first estimate of the flood wave attenuation time was calculated to be 2.04 hours.

The second iteration incorporated this new value, recalculating to 3.5 hours. The updated total rainfall and runoff volumes rose to 92.9 mm and 5.23 million m³, respectively, while the average discharge reduced to 661.2 m³/s due to the longer base time.

A third iteration was conducted using the newly obtained 2.32 hours, resulting in a final time of 3.8 hours. The corresponding rainfall, runoff, and discharge values were 93.7 mm, 5.36 million m³, and 635.0 m³/s, respectively. The change in attenuation time between the second and third iterations was just 1.3%, indicating convergence, as the variation was below the 5% threshold commonly accepted in hydrological modelling (TRRL, 1981).

The final peak design flow for the 100-year return period was then calculated using a peak factor of 2.8, appropriate for catchments with K<0.5. This resulted in a design peak discharge Q_{100} of 1,777.9 m³/s. These findings emphasise the importance of iterative refinement in empirical flood modelling, particularly in regions with variable catchment characteristics and rainfall regimes. Moreover, the use of an area reduction factor and runoff coefficients tailored to regional hydrological conditions significantly enhances the reliability of design flood estimates (Fiddes, 1976; Ministry of Works, 2007).

3.4 Hydraulic Analysis

Based on the hydrological analysis, the river's peak design discharge was determined to be 1,777.90 m³/s using the TRRL method, with a corresponding mean flow velocity of 8.1 m/s, typical for moderate-to-steep gradient rivers in East African contexts (Fiddes, 1976; Ministry of Works, 2007). To determine the necessary cross-sectional area of the bridge opening, the continuity equation was applied, yielding 219.5 m².

In the proposed design, the bridge comprises five openings, each with a span width of 10 m. The required depth per opening to meet the total cross-sectional flow area was computed to be 4.93 m. Rounding this to a practical construction dimension gives 4.5 m.

To accommodate flood resilience and maintain structural safety, a minimum flood clearance of 1 m is mandated, consistent with bridge design recommendations in tropical flood-prone regions (TRRL, 1981; AASHTO, 2018). This adjustment increases the total required structural depth to 6 m. Therefore, the redesigned bridge configuration comprises five rectangular openings, each measuring 10 m (width) × 6 m (depth), yielding a

total effective flow area that satisfies hydraulic and clearance requirements.

3.5 Comparative Analysis of Hydraulic Capacity: Existing vs. Reviewed Bridge Structure

3.5.1 The Existing Structure

The existing segmental masonry arch bridge comprises four openings, each measuring 10 m in width and 5 m in depth, resulting in an individual cross-sectional area of 50 m². The hydraulic capacity was evaluated using the Manning equation, which resulted in a discharge per opening of 374.39 m³/s. With four such openings, the total discharge capacity of the existing structure is approximately 1,497.57 m³/s. This was sufficient for past hydrological regimes but may no longer meet current or future demands under evolving climate conditions (TRRL, 1981; Ministry of Works, 2007).

3.5.2 Reviewed Structure Design

The revised bridge design, intended to accommodate increased flood intensity, consists of five openings, each measuring 10 m wide and 6 m deep. Using the same Manning formula with updated parameters, the discharge per opening is calculated as 485.97 m³/s. The total hydraulic capacity for the reviewed structure is therefore 2,429.85 m³/s, significantly exceeding the updated 100-year return period design peak discharge of 1,777.90 m³/s derived from TRRL flood modelling (Fiddes, 1976; AASHTO, 2018). This provides a hydraulic safety margin, ensuring long-term flood resilience.

3.5.3 Comparative Design Review and Recommendations

The structural enhancements are intended not only to increase hydraulic capacity but also to improve resistance to debris impacts, scouring, and climate-induced hydrological extremes (Table 1).

Table 1

Hydrology Study, Hydraulic Analysis and Design of the Existing Structure

No.	Existing Structure	Reviewed Structure
1	Peak discharge capacity: 1,497.57 m³/s	Peak discharge capacity: 1,777.90 m³/s
2	Size: 10 m × 5 m × 4 openings	Size: 10 m × 6 m × 5 openings
3	No cutoff walls provided	Cutoff walls ≥ 2.6 m depth recommended
4	Underpinning is applied to only one pier	Strengthening of all erosion-prone piers is advised
5	Approaches lack flood protection	Retaining walls are recommended for embankment stability
6	Piers obstruct debris during floods	V-shaped piers are proposed to allow debris passage

4.0 Conclusion

Field investigations revealed pronounced erosion at the embankments and central piers of the existing bridge, with scour depths reaching approximately 2.0 meters—alarmingly close to the maximum tolerable scour depth of 2.6 meters, beyond which structural integrity could be compromised. This level of degradation poses a critical risk to the load-bearing capacity of the bridge, particularly at the foundations of piers, where scour-induced undermining may lead to instability and eventual collapse if not addressed. The study identified an urgent need for reinforcement measures to prevent further erosion and enhance structural resilience. Recommended interventions include underpinning the affected piers and installing deep cut-off walls with protective aprons to control the progression of scour. In addition, the construction of reinforced retaining walls is necessary to stabilise embankments and limit future hydraulic erosion.

Given the dynamic nature of flood-prone river systems, the importance of routine inspection and long-term monitoring is underscored. Particular attention should be paid to tracking scour depth, sediment accumulation, and overall substructure health after significant flood events. Regular maintenance protocols must be institutionalised to ensure early detection and remediation of erosion-related vulnerabilities. Furthermore, given the increasing flood risks associated with climate change, bridge infrastructure must be redesigned to incorporate adaptive capacity. Future-proofing strategies should incorporate predictive flood

modelling, GIS-based hazard mapping, and elevated design discharges reflecting higher return period events (IPCC, 2021).

5.0 Recommendations

To address the critical vulnerabilities identified in the structural and hydraulic performance of the existing bridge, a comprehensive set of reinforcement and resilience measures is recommended. Immediate structural interventions should prioritise the underpinning of scoured piers and the installation of deep cut-off walls extending beyond the maximum allowable scour depth of 2.6 meters. Protective aprons composed of riprap or concrete should be added around pier foundations to mitigate further erosion. To stabilise the embankments, reinforced retaining walls should be constructed, and erosion-resistant treatments such as geotextile coverings or vegetative stabilisation should be applied to vulnerable slopes.

Hydraulic improvements include reshaping upstream pier profiles into V-shaped configurations to reduce turbulence and facilitate the passage of debris during flood events. Additionally, the bridge's flow capacity should be reassessed using updated hydrological models that reflect climate-induced shifts in peak flood frequencies and magnitudes. Establishing a robust monitoring and maintenance program is crucial—this should involve periodic inspections, particularly after extreme weather events, and the deployment of scour monitoring systems to detect early signs of foundation degradation. Finally, long-term resilience planning must incorporate climate adaptation strategies, including the use of high-resolution GIS-based flood mapping and designing infrastructure to accommodate return period discharges of 100 years or more, in line with emerging climate change projections (IPCC, 2021).

6.0 Acknowledgements

7.0 Funding Statement

8.0 Declaration of Conflicting of Interests

The authors declare that there is no conflict of interest regarding the publication of this paper.

9.0 References

American Association of State Highway and Transportation Officials (AASHTO). (2018). AASHTO LRFD Bridge Design Specifications (8th ed.).

Cheng, Y., & Taylor, M. (2019). Assessment and rehabilitation of historical masonry bridges. Engineering Structures Journal, 188, 400–412.

Clarke, S. (2013). *Surveying and mapping for bridge design*. Wiley.

Ettema, R., Ozkan-Haller, H. T., Mostafa, S., & Ettema, R. (2010). Allowable limit contraction and abutment scour at bridges. Texas A&M Transportation Institute.

Federal Highway Administration (FHWA). (2001). Hydraulic Engineering Circular No. 18: Evaluating scour at bridges (4th ed., Publication No. FHWA NHI 01-001). U.S. Department of Transportation.

Fiddes, D. (1976). Design of small dam catchments in East Africa. Transport and Road Research Laboratory Report.

Gerges, M., Elias, M., & Farghaly, A. (2020). Improving the resilience of bridges in flood-prone areas: A review of strategies and technologies. *Journal of Civil Engineering and Management, 26*(3), 233–245. https://doi.org/10.3846/jcem.2020.10258

Intergovernmental Panel on Climate Change (IPCC). (2021). Climate Change 2021: The Physical Science Basis. Contribution of Working Group I to the Sixth Assessment Report of the Intergovernmental Panel on Climate Change. Cambridge University Press. https://www.ipcc.ch/report/ar6/wg1/

Izdori F. and Katambara Z. (2022), Contribution of Land Use and Land Cover Change to Flooding in Mbeya City", MUST Journal of Research and Development, MUST, Vol. 2no. 1pp. 419-427

Jiao, W., He, J., & Yang, S. (2021). Effects of extreme weather events on the resilience of

transportation networks: A global perspective. *International Journal of Disaster Risk Reduction, 58*, 102134. https://doi.org/10.1016/j.ijdrr.2021.102134

Jones, L. M., & Kumar, S. (2018). Bridge foundation performance under flood-induced scouring. Journal of Bridge Engineering, 23(4), 123–134.

Kashaigili, J. J., Mwakalila, S. S., & Senga, S. R. (2020). Hydrological modeling of seasonal floods in the Rufiji Basin: Implications for infrastructure planning. *Water Resources Management, 34*(5), 1325–1341. https://doi.org/10.1007/s11269-020-02628-0

Katambara Z. (2020), Anti-overturning response of the Naming'ongo Birdge due to wood debris., Journal of Institution of Engineers, The Tanzania Engineer Vol. 17(2) 27-33, ISSN: 0856-0196.

Migliorini, S., Lamberti, L., & Ferrari, L. (2020). Impact of flooding on bridge infrastructure: A case study of vulnerable regions. *Journal of Infrastructure Systems, 26* (4), 04020040. https://doi.org/10.1061/(ASCE)IS.1943-555X.0000532

Ministry of Works. (2007). Hydrological design manual for rural roads. Government of Tanzania.

Mswada, G., Manya, S., & Nguvau, M. (2020). Assessment of structural failures due to flooding in Tanzania: Focus on river bridges. *Journal of Disaster Risk Management, 15*(1), 115–126. https://doi.org/10.1016/j.jdrm.2020.04.005

Nyong, A. O., Adesina, F., & Olomola, A. S. (2007). The effects of climate change on agriculture in Nigeria: A review. *Global Environmental Change, 17*(2), 172–181.

Prokon. (2025). *Prokon Structural Analysis and Design Suite* [Software]. Prokon Software Consultants.

Rezaizadeh, A., Washer, G., & Phares, B. (2011). "Use of Digital Imaging for Bridge Condition Assessment." Journal of Bridge Engineering, 16(6), 753–763.

Sharma, S., Kumar, P., & Rawat, A. (2021). Flood-induced erosion and its impact on bridge structures in riverine areas: A case study of Indian bridges. *Environmental Engineering Science, 38*(4), 291–302. https://doi.org/10.1089/ees.2020.0536

Smith, A. J., Brown, D., & Ali, H. (2020). Flood risk and infrastructure vulnerability in riverine bridge systems. Natural Hazards Review, 21(3), 150–161.

Swilla, L., Katambara, Z., & Lingwanda, M. (2024). Quantifying suitable low-impact development practices in mitigating runoff floods for the Kinyerezi River catchment in Dar es Salaam, Tanzania. Water Practice & Technology, 19(7), 2868-2882.

Texas Department of Transportation. (2018). Scour evaluation guide. TxDOT.

Transport and Road Research Laboratory (TRRL). (1981). Overseas Road Note 4: Road design for tropical and sub-tropical countries. TRRL, UK.

U.S. Geological Survey. (2025). Bridge scour. In Wikipedia. Retrieved from https://en.wikipedia.org/wiki/Bridge_scour

United Republic of Tanzania (URT). (2015). *National adaptation programme of action (NAPA) to climate change*. Ministry of Environment.

Wang, X., Zhang, M., & Liu, Y. (2020). Impact of hydraulic forces and scouring on bridge foundations in flood-prone regions. *Journal of Hydrology, 585*, 124792. https://doi.org/10.1016/j.jhydrol.2020.124792

Zhao, Y., Wang, Y., & Xie, H. (2019). Assessing the vulnerability of transport infrastructure to flooding: Case studies and solutions. *Engineering Structures, 198*, 109421. https://doi.org/10.1016/j.engstruct.2019.109421